

Detection of surface-laid mine fields in VNIR hyperspectral high spatial resolution data

Steven B. Achal^a, Clifford D. Anger^a, John E. McFee^b and Robert W. Herring^b

^aItres Research Ltd.,
155, 2635 - 37th Avenue NE, Calgary, Alberta, Canada T1Y 5Z6

^bThreat Detection Group, Defence Research Establishment Suffield,
Box 4000, Station Main, Medicine Hat, AB, Canada, T1A 8K6

ABSTRACT

The feasibility of detecting surface-laid and, in some circumstances, buried mines by analysis of visible to near-infrared (VNIR) hyperspectral imagery has been demonstrated by the authors in previous studies. An important factor in the practical success of such technology is being able to achieve the necessary spatial and spectral resolution to allow discrimination of mines from background. With some restrictions, both can be improved by increasing the instrument data output rate or decreasing the platform speed and both can be traded off against one another. The optimum trade-off must be determined for a given problem, including the choice of algorithm.

Airborne VNIR hyperspectral data were collected over several controlled surface-laid mine fields using a *casi* hyperspectral imager and a helicopter. The combination of the imager's high speed data recording coupled with the low airspeed of the helicopter enabled the collection of hyperspectral data ranging from four 136 nm wide spectral bands at 10 cm resolution to nine 60 nm wide spectral bands at 20 cm resolution. Each mine field contained a variety of mines ranging from small anti-personnel mines to large anti-vehicle mines. An assessment of the feasibility and practicality of using airborne hyperspectral data to detect various surface-laid mines and mine fields was conducted. In addition, the trade-offs between spectral and spatial resolution for the detectability of surface-laid mines and mine fields are discussed.

Keywords: Mine detection, Hyperspectral imaging, Visible, Infrared, Reflectance

1. INTRODUCTION

The Defence Research Establishment Suffield (DRES) and Itres Research Ltd. have been collaborating since 1989 to develop a mine detection capability using hyperspectral imaging. The feasibility of detecting surface-laid mines using a near-nadir, visible/near infrared (VNIR) wavelength hyperspectral imager was first demonstrated in experiments conducted between 1989 and 1994 at DRES and Canadian Forces Base Calgary, Alberta, Canada.¹ A DRES-owned *casi* imager, manufactured by Itres, was used to obtain high spatial resolution hyperspectral radiometric images of replica mines and backgrounds. The instrument (Fig. 1), which operates in the 400-1000 nm waveband, uses a diffraction grating to spread a slit image across a two dimensional charge coupled device (CCD), producing a spectral vector of up to 288 elements for each pixel of the image.² Being a pushbroom imager, horizontal motion is required to build up one dimension of the image. This was done by horizontally scanning the instrument close to the ground (~6 m altitude) from a personnel lift at a scan speed of 0.1 m/s or less. Both spectral mode images with high spectral resolution (up to 4 nm) and spatial mode with fewer, broader bands, but higher spatial resolution (up to 4 mm), were obtained. The radiance images were converted to reflectance images using a calibrated reflectance panel. It was also found that under certain conditions, an incident light sensor (ILS) which measures downwelling solar radiation, could be used to convert image radiance to a good approximation to reflectance. A variety of simulant and replica mines were distinguished from a variety of background types with probabilities near 100%, for widely varying illumination conditions caused by diurnal and seasonal variations, sky conditions and sun angles. The imager was even able to detect mines partially obscured by vegetation. General waveband ranges were determined from high spectral resolution data and were found to give good classification results.

Other author information: (Send correspondence to J.E.M.)

S.B.A., C.D.A.: Email: stevie@itressun.itres.com, cliff@itressun.itres.com; Telephone: 403-250-9944; Fax: 403-250-9916

J.E.M.: Email: John.McFee@dres.dnd.ca; Telephone: 403-544-4739; Fax: 403-544-4704

R.W.H.: Email: Robert.Herring@dres.dnd.ca; Telephone: 403-544-4048; Fax: 403-544-4704



Figure 1. *casi* hyperspectral imager. At left from top to bottom are the monitor, control unit and power supply. At right rear is the sensor head.

Airborne images of a simulated mine field were first obtained at Vulcan, Alberta, Canada in July 1994.³ Surrogate mines made of 0.8m x 0.8m green indoor-outdoor carpet were laid in rows in a series of agricultural fields containing different crops. The carpets were quite difficult to distinguish from the vegetation with the human eye. The fields were overflowed by the *casi* in a fixed wing aircraft at 56.6 m/sec (110 knots) at an altitude of 300m. The *casi* used was state-of-the-art at that time. It employed a new high performance custom objective lens, a fast readout system (880Kbytes/sec), dual Exabyte drives, and an enhanced spectral mode which was capable of providing full spatial resolution along with complete spectral information. Six 20-30 nm bands, from 520-720 nm were used in spatial mode and sixteen 32 nm wide bands with 256 adjacent look directions were used in spectral mode. This yielded a pixel size of roughly 1.6m x 0.5m, whose area was slightly greater than the target area. Conversion to reflectance was done using an ILS, mounted on the aircraft and checked against a calibrated reflectance tarp. Although good detectability was observed where carpets were known to be, high winds blew away some of the carpets, preventing proper ground truthing. Thus, accurate probability of detection (Pd) and false alarm rate (FAR) could not be determined.

DRES and HDI of Dartmouth NS, Canada have also used the *casi*, horizontally scanned near the ground from a personnel lift, to detect buried mines.^{4,5} The mines were indirectly detected by observation of differences in reflectance spectra between compact regions over top of mines and regions of background materials. The differences were thought to be caused by disturbed versus undisturbed vegetation and surface soil, vegetative stress due to mine implantation even if the surface was apparently undisturbed, and/or vegetative stress due to explosive vapours originating either from leaks in the mine case or from residue contaminating the case. Surrogate mines and blocks of explosive were buried under various vegetative covers and bare soil using standard mine laying methods. Images were obtained at various times from 1 2/3 to 15 1/2 months after burial. Mines under short and medium length vegetation and bare soil were detectable by calculating the linear correlation coefficient or fractional composition, derived from orthogonal subspace projection, for each pixel of the image. The probability of detection for surrogates decreased with increasing vegetation length and appeared to vary somewhat with environmental conditions. Short vegetation gave better detection results than bare soil which gave better results than medium length vegetation. Pd was typically in the range of 55 to 94% and FAR varied from about 0.17 to 0.52 m⁻². There were insufficient data to assess the relative importance of stress due to explosive vapour leaching into the soil compared to stress induced

by soil disturbance.

2. MEDIUM RESOLUTION EXPERIMENT

2.1. Experimental description

Generally, target detection algorithms perform better as the target fills more of the area of the pixel. Thus, the most straightforward way to improve performance is to increase the spatial resolution. In an effort to obtain data with pixel sizes less than the width of a surrogate mine, a second airborne experiment was conducted at a site near Canmore, Alberta, Canada on September 28 1994. Squares of the same indoor-outdoor carpet used in the Vulcan experiment were placed in two roughly parallel rows separated by approximately 15 m. Each surrogate mine was 0.8m x 0.8m and was separated by approximately 25 m from the next one in the row. Two 5m x 5m brown reflectance tarps were also laid near the two rows of targets. The Vulcan data were obtained with a *casi* that was state-of-the-art at that time. The across track spatial resolution, which is a function of the optics and altitude, could be improved by decreasing the altitude, at the expense of decreased swath width. Since the across track pixel size was already less than the width of the targets, there was no need to change the altitude.

The along track resolution is a function of CCD readout speed, integration time, number of bands and platform velocity. It could be improved by using a slower platform. To achieve this, the *casi* was flown on a helicopter at a speed of 18.0 m/sec (35 knots) over the surrogate mine field at an altitude of 300 m. Enhanced spectral images using sixteen 32 nm bands and 256 look directions were obtained with a spatial resolution of 0.5 m x 0.5 m.

2.2. Analysis

Raw image data units were corrected for electronic offset, dark current, scattered light and frame shift smear and then converted to spectral radiance units using ITRES calibration software. The incident light sensor could not be used in this experiment due to mechanical constraints of the helicopter. Instead the previously measured reflectance properties of the calibration tarps were used to convert the spectral radiance values into reflectance. The reflectance spectra of mines in the 500 to 680 nm band, estimated in this manner, have been shown to be independent of diurnal and seasonal illumination variations to within an offset and scale factor.¹

Reference reflectance spectral vectors, or “design set” vectors, were obtained from laboratory measurements of the targets under known, controlled lighting. Two classifiers were used in this study, both of which had been previously successful in detecting surface-laid mine replicas and surrogates and buried mine simulants in *casi* images.^{1,3-5}

The linear correlation coefficient (LCC) is a measure of similarity between an unknown spectral reflectance vector and a reference vector, computed for each pixel on an image. It can be shown¹ that the LCC is insensitive to the spectral scale and offset factors exhibited by the estimated reflectance spectra of experiments such as these. End member analysis, or spectral unmixing, and spectral angle mapping, which is a special case of the LCC, do not generally have this property.

LCC classification relies on the spatial resolution being sufficiently high so that individual pixels contain essentially only one material. This would not be the case for some of the on-target pixels at the medium spatial resolution of the Canmore experiment. Spectral unmixing techniques do not have this restriction. A particularly suitable method for this problem is orthogonal subspace projection (OSP), which was used in the Vulcan experiment to detect subpixel extent targets.³ OSP assumes a linear mixing model in which the spectral reflectance vector at a given spatial position is the weighted sum of the reflectance vectors of the materials (end members) found within the pixel, with weights given by the area fractional composition of the materials. The measured spectral vector is projected onto a subspace which is orthogonal to that which is spanned by the vectors of the background materials.^{6,7} A matrix approximating the latter can be estimated from the covariance matrix of the image under the assumption that the fraction of the image corresponding to target areas is small. This optimally nulls the composite background material vectors in a least squares sense. The fractional composition (FC) of the target material for each pixel can then be estimated by a set of matrix operations³ and an image of FC values formed.

LCC and OSP images were contrast stretched and enhanced by a number of standard techniques, such as linear, Gaussian, histogram equalization and square root stretches and level slicing, available from the ENVI hyperspectral image processing software.⁸

2.3. Results and discussion

An image set from the Canmore experiment is shown in Fig. 2. The upper left image is a three colour composite image (printed in grey scale) of a portion of the flight line containing surface-laid surrogate mines. The surrogates are invisible to the unaided eye on the full colour image, even when inspected at highest magnification. The upper right image is a single band image of the same region processed from the original 16 band image using the OSP classifier, followed by contrast stretching and thresholding. The threshold was selected to eliminate as much of the background as possible, while still retaining all detected targets. Each circled white cluster of pixels is a surrogate mine target. All targets are detected, although a number of false alarms are visible as well. The lower left image is the corresponding single band image processed from the original 16 band image using the LCC classifier, followed by contrast stretching and thresholding. All targets were again detected. False alarms are present, but are not as numerous as for the OSP image and not always correlated with those in the OSP image. The lower right image is the pixel by pixel product of the OSP and LCC images, stretched and thresholded. All targets are still detected, but false alarms have been dramatically reduced.

Given the small sample size, estimates of Pd and FAR must be viewed with caution. With this caveat in mind, an estimate of Pd and FAR for the product image was attempted. A detection was first defined to be a cluster of between 2 and 5 pixels exceeding the threshold of the classified image. The probability of detection of individual mines for this image is 100% and no false alarms are present. If the detection condition is relaxed to include single pixels above threshold, 12 false alarms are present. The area of the image is approximately 38400 m², yielding a worst case FAR of 0.00034 FA/m².

3. HIGH RESOLUTION EXPERIMENT

3.1. Introduction

The previously described ground based and airborne experiments showed promise, particularly for surface-laid mines, but a number of issues had to be resolved. In the above experiments, images were processed and analysed off-line within a few days of collection. This is acceptable for humanitarian de-mining, but it is not so for many military applications. Part of our ongoing work has thus been aimed at modifying the DRES *cas*i to allow real-time processing of the raw image data. This is difficult, since it requires processing the entire data stream from raw image through radiometric correction, conversion to reflectance, and generation of spectrally classified imagery. Besides processor hardware development, work is being done on modification of the currently used classification algorithms, such as the linear correlation coefficient and orthogonal subspace projection, and selection and development of new algorithms that are suitable for implementation in real-time.

The ability to process images spectrally in real-time opens up the possibility of applying spatial processing to the spectrally processed images. Research by DRES and the University of British Columbia⁹ has led to a hierarchical algorithm that has the potential to detect scatterable and pattern mine fields. The full algorithm requires single band images, which the LCC, OSP or product provide. The algorithm performs better if shape analysis can be performed on the individual detected targets. This requires sufficient spatial resolution so that a mine spans at least several pixels. This condition was met in the Medium Resolution experiment, but only because the surrogate mines were much bigger than real mines. Typical anti-tank (AT) mines are 30 cm in diameter, whereas anti-personnel (AP) mines can have widths of 10 cm or less. It was thus felt that higher spatial resolution was needed and continual improvements have been made to the instrument toward this goal.

Another consideration was the desire to test airborne detection capability against real mines. Real mines are, of course, substantially smaller than the oversized surrogates used previously, which increases the instrumental challenge. Mine paints and coatings may be substantially different spectrally than the airborne surrogates and the replica mines used in the ground based experiments. Mines have various two dimensional shapes and also have three dimensional surface structure, which is more likely than the flat surrogates to provide a specular component of reflection. One must be very cautious when extrapolating the results of surrogate and replica target experiments to real mines. At the same time, it was desired to create a spectral library of VNIR mine reflectances in the laboratory, to see if laboratory generated spectral design sets would perform as well as ones generated *in situ*. If successful, this could substantially decrease the effort required in surveying a suspected mined area.

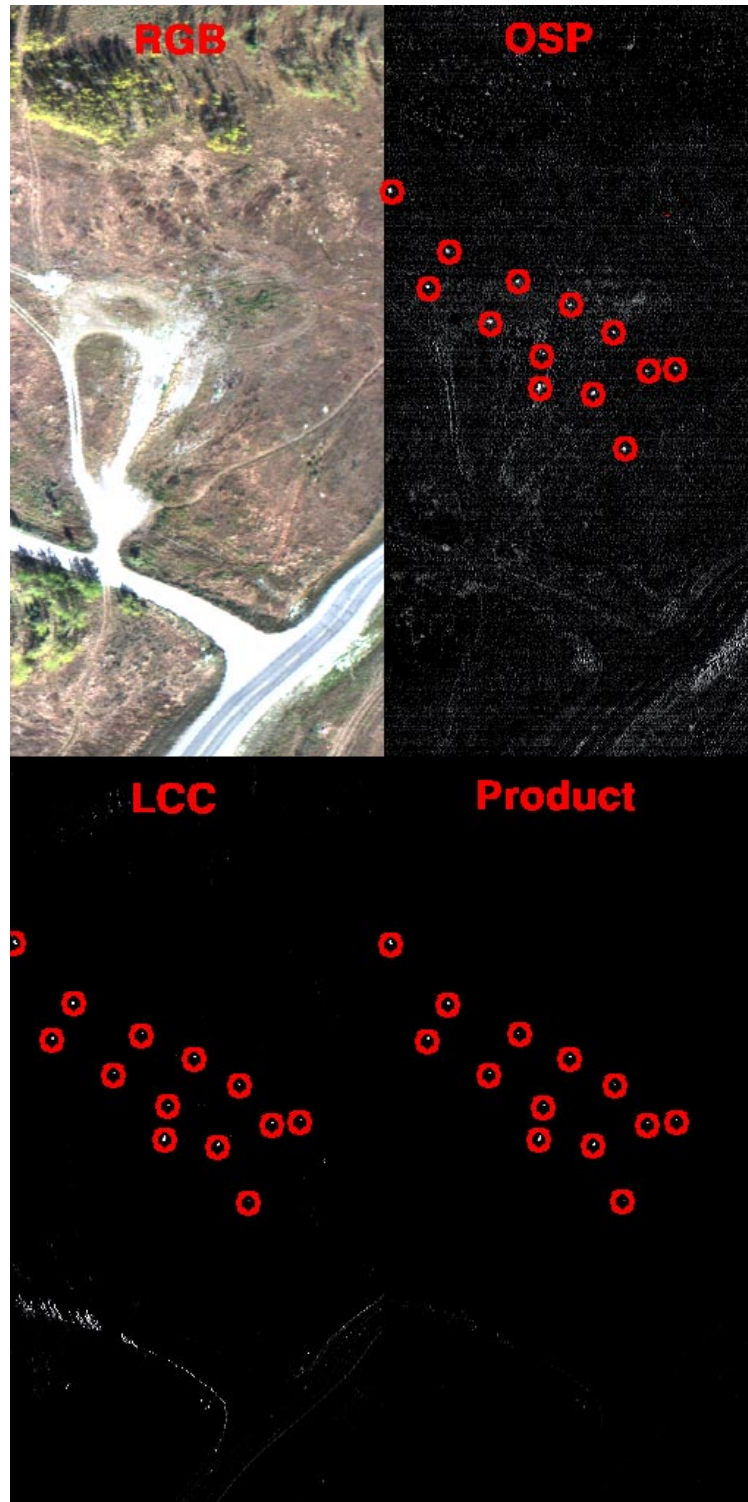


Figure 2. Airborne *casi* image of a field of surface-laid mine surrogates. Upper left image is a conventional 3 colour image (printed in grey scale) of the area. Mines widths are a few pixels wide and the mines are invisible on the full colour image. The upper right and lower left images are single band images of the same scene, obtained by processing the 16 band *casi* image with the OSP spectral classifier and LCC classifier, respectively. The lower right image is the product of the two classified images. Each circled bright blob is a mine.

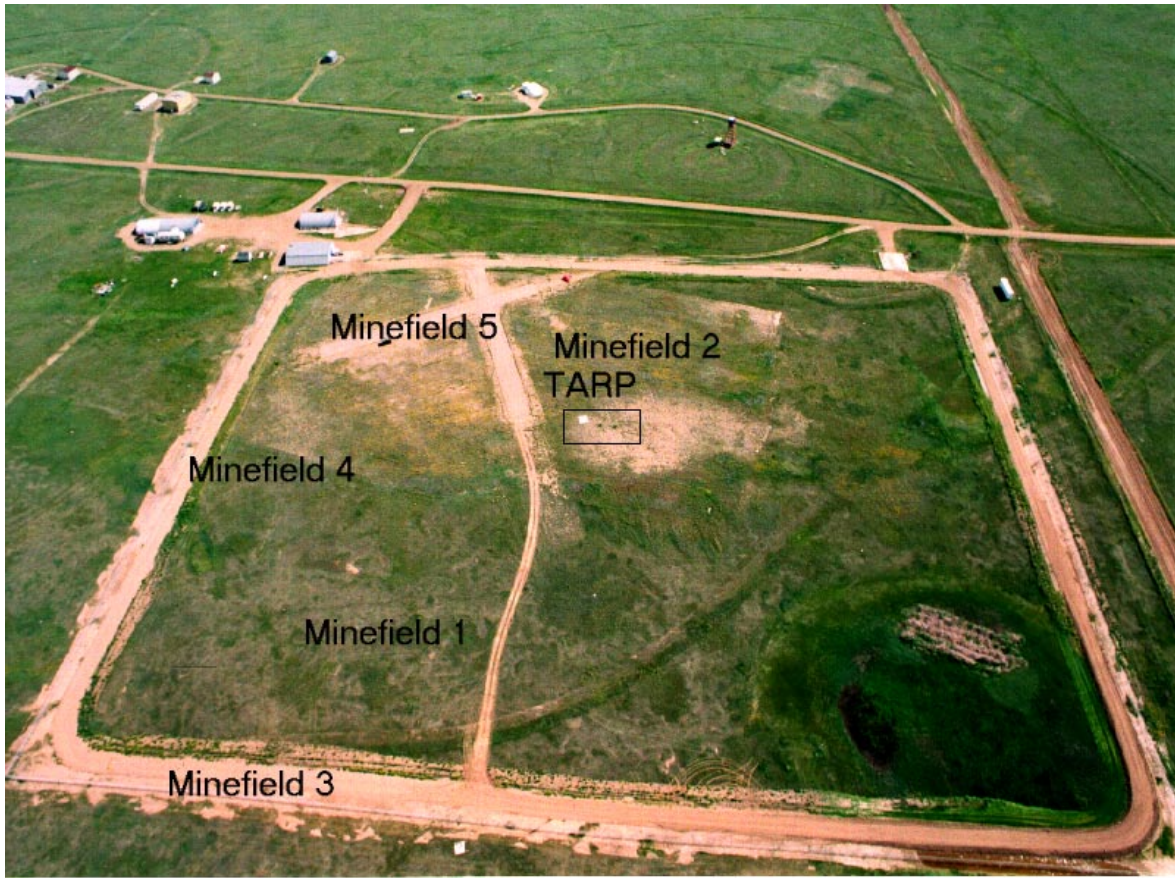


Figure 3. Aerial image of the DRES Mine Pen. Each numbered area corresponds to a different mine field.

3.2. Experimental description

In order to test improvements in the *casi* instrument and its performance against real surface-laid mines, an experiment was carried out at the DRES Mine Pen on June 19 1997. The Mine Pen, shown in Fig. 3, is located on the DRES Experimental Proving Ground at approximately $50^{\circ}17.57'$ north $111^{\circ}06.95'$ west. The rectangular area, which is roughly 260 m by 340 m, encloses a 1.1 kilometer perimeter dirt road, two 100 m asphalt strips and a variety of short and long vegetation. Mines can be placed on or under the ground surface and left for extended periods of time. Mine fields were surface-laid in 5 areas of different ground surface types (Table 1). Thirty different types of mines were used, including 11 real anti-tank mines, 10 real anti-personnel, 6 replicas and 3 simulants (Table 2). Reference stakes were put in the ground for each mine field at 20 or 25 m intervals and their positions were measured the day after the experiment using a differential global positioning system (DGPS) with a 20 cm accuracy. The morning of the experiment, mines were laid out at 5m intervals along a straight line or on a rectangular grid by measuring from the stakes with a tape measure. A tarp of known reflectance was laid out in the center of the Mine Pen to facilitate conversion from radiance to reflectance.

The *casi* was mounted in a helicopter to look directly downward. A roll correction gyroscope and DGPS receiver were mounted in the helicopter to enable geocorrection of the imagery. To handle the high data readout rates necessary to achieve such high spatial resolution, data were stored on 3 interleaving Exabyte 8500 tape drives for postprocessing. The mine fields were overflown at an airspeed of 18.0 m/sec (35 knots) between 14:00 hours and 16:00 hours local time. A number of different band sets were used in both spatial and spectral mode (Table 3). For each band set, band widths were roughly constant across the wavelength range. Contiguous bands were used since previous experience had shown that the OSP algorithm requires contiguous bands spanning a significant spectral range of at least 300 nm, whereas the width of the bands has only a small effect on algorithm performance. Altitudes were varied for each band set to achieve square pixels. In order to facilitate estimation of scene reflectance, images

Mine Field Number	Surface Cover Description	Mine Field Shape	Mine Field Dimensions (m)	Total Number of Mines
1	medium length green grass, scrub	rectangular grid	20 × 25	30
2	medium length yellowish green grass, scrub	rectangular grid	20 × 25	30
3	well packed dirt road	1 line	140	29
4	dense green scrub	1 line	125	26
5	asphalt	2 parallel lines	55,45	22

Table 1. Mine fields for high resolution experiment. All mines were spaced 5m apart.

were recorded only when clouds did not obscure the sun. Moderate gusting winds yielded high, variable crab angles (yaw angle relative to flight line) that were typically 20-30° and as high as 45°.

3.3. Analysis

Interleaved data on multiple tapes were collated using Itres software onto a single tape of raw image data. Conversion of the raw image data units to spectral radiance units was accomplished as before. Radiance units were again converted to reflectance units by means of the known reflectance tarp. The tarp was not in each image, but images without tarps were taken within a few minutes of the ones with the tarp. The variation in sun angle during that time was not significant in the estimation of reflectance. Since all images were taken only when clouds did not obscure the scene of interest, the conversion to reflectance should be valid.

Reflectance calibration was also attempted using the incident light sensor (ILS). This is a skyward-looking cosine diffuser which provides a signal at the instrument entrance slit which is proportional to the down welling solar radiation. The ILS values for a particular image line are stored in the last row of CCD pixels for the line. The ILS values, together with a knowledge of the sun angle when the image was acquired, can be used to convert the radiance image into a reflectance image.

Geocorrection was accomplished by means of DGPS and pitch/roll gyroscope information recorded with the raw image data, together with information recorded at a DGPS base station situated beside the Mine Pen. Yaw angles were estimated based on the known flight line direction and observed crab angles.

Design set spectra were extracted from the ground truthed reflectance images of the north road (area 3), since these were the easiest images in which to unambiguously identify some mine locations. Spectra for those locations were extracted and put into a spectral library using ENVI. They were used in subsequent classification of the images from all areas. Only anti-tank mines were large enough to provide pixels with pure spectra and hence only AT mine signatures were put in the library.

In order to test the practicality of using ground based spectral measurements to generate spectral libraries for airborne classification, hyperspectral images of a wide variety of mines were obtained using a ground based *casi* on June 24, 1998. The instrument was placed on a pan/tilt assembly on a tripod, a few meters from each mine. Immediately beside each mine was a calibrated reflectance panel. Images were formed by manually scanning the *casi* field of view across the mine and panel. Images were taken in either sunlight or quartz halogen light. The same band sets used in the airborne experiment were used, as well as a high spectral resolution set (72 bands, 7.5nm wide). Conversion to reflectance units was accomplished as in the airborne experiments, by means of the reflectance panel. Reflectance spectra were extracted from the mines and put into spectral libraries using ENVI.

Again the LCC, OSP and product of the two were used as spectral classifiers. Images were contrast stretched and enhanced by various standard techniques.

3.4. Results and discussion

The analysis of the high resolution data is still in a preliminary stage and the ground based signatures have not yet been completely extracted and compiled into libraries. Thus, the aerial libraries were used in the subsequent analysis. The chief reason for the delay is that since the July 1997 experiment, there has been a substantial diversion of effort toward the high priority development of a teleoperated, vehicle mounted, multisensor landmine detector under the Improved Landmine Detector Project (ILD).¹⁰ A significant component of the *casi* work has been aimed

Mine Name	Type	Shape	Largest Dimension (cm)	Color	Cover Material
FFV028	AT	circle	26.0	olive drab (OD)	painted metal
M15	AT	circle	33.7	OD	painted metal
M21	AT	circle	23.0	OD	painted metal
Mk7	AT	circle	32.5	brown	coated metal
TM62M	AT	circle	32.0	OD green	painted metal
NR30	AT	curved rectangle	28.3	olive green	plastic
PT Mi-Ba III	AT	circle	33.0	green,black	plastic
TMA-3	AT	circle	26.5	OD	painted fiberglass
TMA-4	AT	circle	28.0	OD	plastic
TMA-5A	AT	square	31.2	OD	plastic
TMRP6	AT	circle	29.0	light OD green	plastic
FFV013	AP	curved rectangle	42.0	OD	fiberglass
M16A2	AP	circle	10.3	OD	painted metal
M18A1	AP	curved rectangle	21.6	OD	fiberglass
PMA-1A	AP	rectangle	14.0	OD	plastic
PMA2	AP	circle	6.8	OD/light green	plastic
PMA3	AP	circle	10.3	OD,black	rubber,plastic
PP Mi-Sr	AP inert	circle	10.2	OD green	painted metal
Valmara 69	AP	circle	13.0	OD	rubber,plastic
VS-Mk2	AP	circle	9.0	green,black	plastic
VS-50	AP	circle	9.0	OD	plastic
TMN46	AT replica	circle	30.5	OD green	painted metal
PM60	AT replica	circle	32.1	OD green	plastic
TMD-1	AT replica	rectangle	32.0	natural wood	wood
PMN 6	AP replica	circle	11.2	OD	rubber covered plastic
OZM3	AP replica	circle	7.5	OD green	painted metal
PFM-1	AP replica	butterfly	12.0	OD green	plastic
IRAT	AT IR simulant	circle	25.0	dark green	plastic
IRAP	AP IR simulant	circle	10.5	dark green	plastic
DRES Mine	AT training	circle	30.0	OD	plastic

Table 2. Mines used in high resolution experiment. Shape and dimension are in the horizontal plane when normally emplaced.

Band Set name	Spatial Resolution (m)	Mode	Height above ground (m)	Number of bands	Minimum wavelength (nm)	Maximum wavelength (nm)	Range (nm)	Average Bandwidth (nm)
d20cm1	0.20	spectral	150	9	407.3	954.5	547.2	61.8
d15cm1	0.15	spectral	112	6	407.3	954.4	547.1	92.0
d10cm1	0.10	spectral	75	4	407.3	954.5	547.2	137.6
dspat1	0.20	spatial	150	7	481.2	768.2	287.0	42.0
dspat2	0.15	spatial	112	3	499.9	800.9	301.0	101.2

Table 3. Band sets used for high resolution experiment.

at studying its role in ILDP, and additional effort at DRES was expended in subsequent competitive trialing of ILDP in the U.S. Ground-based Standoff Mine Detector System (GSTAMIDS) trials of Summer 1998.

Most of the preliminary analysis has been done on the 15 cm resolution spectral mode imagery. An example is shown in Fig. 4. This is a reflectance image of portions of mine fields 1 and 3, having a spatial resolution of 15 cm. The band shown is centered at 541.8 nm. Some mines are faintly visible to the eye as dark splotches on the main road, where they contrast most sharply with the background. Many are invisible as are all of the ones in the vegetation.

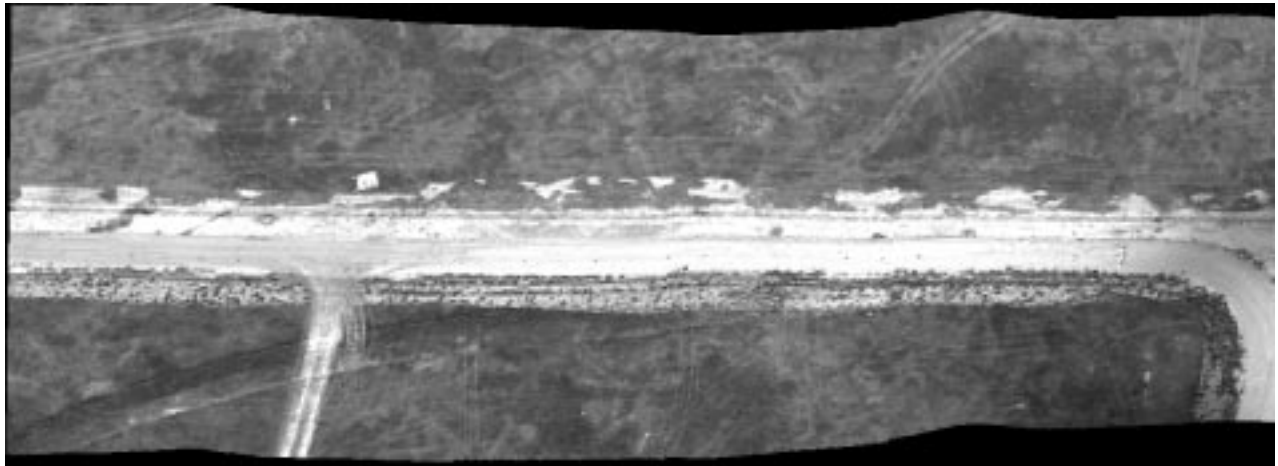


Figure 4. Reflectance image of the 541.8 nm band of portions of mine fields 1 and 3.

Preliminary analyses on the 15 cm spectral mode data showed that, as for the Canmore experiment, the LCC×OSP product gave the best results among the previously described classifiers. It also outperformed a number of standard classifiers available within ENVI. Thus, we will restrict further discussions to that classifier. Fig. 5 is the LCC×OSP product of the same portions of mine fields 1 and 3 as shown in Fig. 4, using the IR simulant AT mine as a template. Circles indicate IR simulant mine locations detected by the algorithm. The squares indicate other mine types detected by algorithm. With a threshold of 0.45, all IR simulant AT targets in the field of view are detected, with roughly 50 false alarms, yielding a FAR of 0.0043 FA/m². Unfortunately, the IR AT simulant was the only mine which had multiple copies in the field of view. Some other AT mines (the only ones with available design set spectra) were tried and were detected, but this is expected since the design set spectrum in this case is identical to the test spectrum.

A number of factors conspired to make ground truth information less reliable than was necessary to provide accurate Pd and FAR values for all the mine fields. The high value and variation of aircraft crab angles caused substantial errors in yaw angle estimation. The subsequent geocorrection then produced significant errors in pixel placement and gaps in the flight path coverage. These gaps, together with an insufficient density of clearly visible control points, made it difficult to determine accurately where the individual locations of all the targets were on the images, even though the geographical locations of the mines were known from DGPS. However, visual cues and the regular arrangement of the mines did allow determination of the mine locations in some cases.

Generally, detection and false alarm rates were similar on the asphalt and the dirt road, due to the relatively large spectral difference between the mines and backgrounds. Within ground truth uncertainties, mines appeared to be identifiable in the medium length yellow green grass cover of mine field 2. However, no mines were detected in mine field 4 which had dense green scrub brush. Given the ground truth problems and limited target set, it is difficult to draw strong conclusions from this.

A detailed tradeoff study of the number and width of spectral bands versus number and size of spatial pixels has been hampered by saturation problems in some bands for a number of band sets, and is not yet complete. An initial look indicates that 3 or 4 broad bands lack sufficient resolution to adequately separate the spectral vectors of the mines from the background. However, many of the false alarms are single pixels. The higher spatial resolution afforded by reduced numbers of bands would help eliminate these false alarms, by allowing the use of either simple

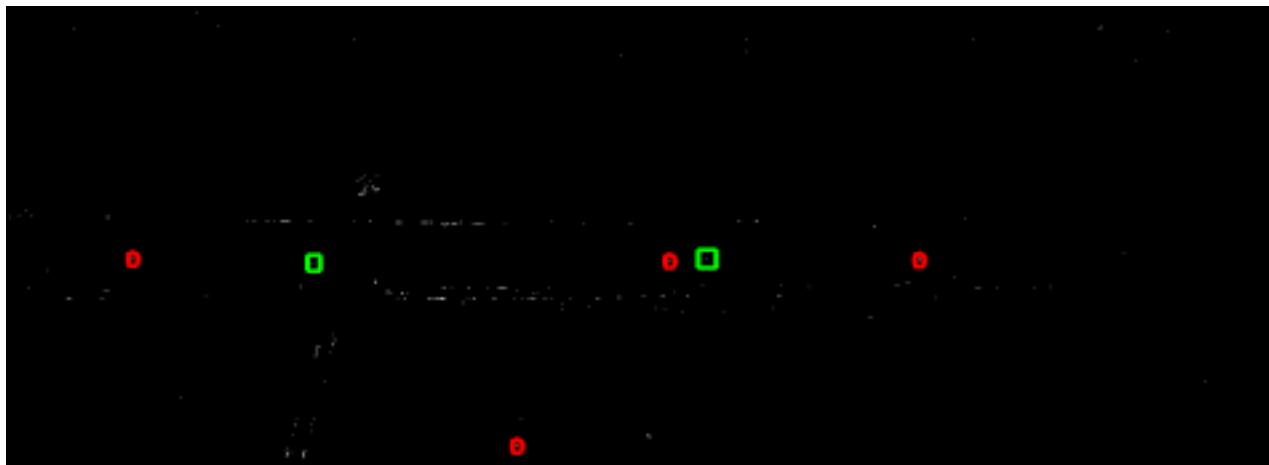


Figure 5. LCCxOSP product of the same portions of mine fields 1 and 3 as shown in Fig. 4, using IR simulant mine as template. Circles indicate IR simulant AT mine locations detected by algorithm. Squares indicate other mine types detected by algorithm.

spatial neighbour analysis or more sophisticated shape analysis algorithms.⁹ From the preliminary work presented here, 15 cm spatial resolution and 6 bands is a reasonable compromise for the AT mines examined here on medium vegetation, dirt and asphalt. Higher spatial resolution will be necessary for AP mines and higher spectral resolution will be needed for dense green vegetation. Obtaining both at the same time will be a challenge, but nevertheless a goal, for instrument development.

4. FUTURE PLANS

A second high resolution experiment is planned at the Mine Pen location in late Spring or Summer 1999. The state-of-the-art in spectral and spatial resolution will be employed. Improved ground truthing will be implemented and full geocorrection will be attempted, using a three axis inertial measurement unit and DGPS. The ground based spectral reflectance reference libraries will be complete by then and will be used in the classification. This should allow accurate Pd and FAR to be obtained for the various ground covers.

For the long term, investigations continue on determining the feasibility of employing a *casi* as a forward looking imager in ILDP or its associated protection vehicle.¹⁰ As a part of this, a mirror stabilization system is being developed and real-time processing of the data is being implemented. Spatial/spectral algorithms which profit from the large number of pixels subtended by a mine are also under development.

Although VNIR hyperspectral imaging shows promise for some mine detection roles, it has some problems. First, the algorithms employed must be run once for each expected mine type. This makes the execution time consuming and implementation cumbersome due to the large spectral library required. The former is not a problem for humanitarian de-mining and may be alleviated for intensive military applications by implementation of real-time processing. Second, the detection of buried mines by VNIR imaging suffers from high false alarm rates.

The short wave infrared (SWIR) and thermal infrared (TIR) bands may alleviate these problems. In general, the wider the overall spectrum available, the less likely it is to have natural or intended false alarms. Also, it becomes more difficult to camouflage a target. More specifically, the pigments and plastics used in land mines contain organic and complex inorganic compounds, which often have significant and unique absorption features in the SWIR. These reflectance spectra may contain both unique and general absorption features, making a mine-specific detection algorithm more viable than those developed for the VNIR, but also making possible a practical generic surface-laid mine detection system. Some research on buried mine detection using TIR hyperspectral imaging¹¹ has indicated that the spectra of certain soils measurably change depending on whether or not the soil is disturbed. It may be possible that this effect extends to other soil compositions and to the SWIR range.

To this end, a program has been initiated in SWIR and TIR hyperspectral imaging of mines. Preliminary work involves measuring the SWIR reflectance spectra of a wide variety of land mines, background materials and the daytime sky using a portable SWIR non-imaging spectrometer. In parallel, because of the significant advances that have occurred in SWIR sensor technology, a project has been started to design and build a SWIR hyperspectral imager which is optimized for mine detection. Prior work on TIR hyperspectral mine detection was done using Fourier Transform spectrometers which are far too slow for practical applications. To obtain the necessary speed improvement, we have started a preliminary investigation into the application of TIR microbolometer array technology to a dispersive hyperspectral imager.

ACKNOWLEDGMENTS

This work was supported by the Research and Development Branch, Department of National Defence, Canada, under Project Number 2mb20.

REFERENCES

1. J.E.McFee, S.Achal, and C.Anger, "Scatterable mine detection using a *casi*," in *Proceedings of the First International Airborne Remote Sensing Conference*, pp. I587–I598, September 1994.
2. C.Anger, S.Mah, and S.Babey, "Technological enhancements to the Compact Airborne Spectrographic Imager (*casi*)," in *Proceedings of the First International Airborne Remote Sensing Conference*, pp. II205–II213, 1994.
3. S.Achal, J.McFee, and C.Anger, "Identification of surface-laid mines by classification of compact airborne spectrographic imager (*casi*) reflectance spectra," in *Detection Technologies for Mines and Mine-like Targets*, A.C.Dubey, I.Cindrich, J. Ralston, and K.Rigano, eds., *Proc. SPIE* **2496**, pp. 324–335, 1995.
4. J.McFee, H.Ripley, R.Buxton, and A.Thriscutt, "Preliminary study of detection of buried landmines using a programmable hyperspectral imager," in *Detection and Remediation Technologies for Mines and Mine-like Targets*, A.C.Dubey, R.L.Barnard, C.J.Lowe, and J.E.McFee, eds., *Proc. SPIE* **2765**, pp. 476–488, 1996.
5. J.E.McFee and H.T.Ripley, "Detection of buried landmines using a *casi* hyperspectral imager," in *Detection and Remediation Technologies for Mines and Mine-like Targets II*, A.C.Dubey and R.L.Barnard, eds., *Proc. SPIE* **3079**, pp. 738–749, 1997.
6. J.C.Harsanyi and C.I.Chang, "Hyperspectral image classification and dimensionality reduction: an orthogonal subspace projection approach," *IEEE Transactions on GeoScience and Remote Sensing* **32**, pp. 779–785, 1994.
7. C.I.Chang, X.L.Zhao, M.L.Althouse, and J.J.Pan, "Least squares subspace projection approach to mixed pixel classification for hyperspectral images," *IEEE Transactions on GeoScience and Remote Sensing* **36**, pp. 898–912, 1998.
8. Better Solutions Consulting Ltd., Lafayette, CO, USA, *ENVI Users Manual*, 3.0 ed., December 1997.
9. M.R.Ito, J.E.McFee, S. Duong, and K.L.Russell, "Pipe-lined algorithm and parallel architecture for real-time detection of sparse small objects in images," in *Signal and Data Processing of Small Targets 1997*, O.E.Drummond, ed., *Proc. SPIE* **3163**, pp. 150–161, 1997.
10. J.McFee, V.Aitken, R.Chesney, Y.Das, and K.Russell, "A multisensor, vehicle-mounted, teleoperated mine detector with data fusion," in *Detection and Remediation Technologies for Mines and Mine-like Targets III*, A.C.Dubey, J.F.Harvey, and J.T.Broach, eds., *Proc. SPIE* **3392**, pp. 1082–1093, 1998.
11. A.DePersia, A.Bowman, P.Lucey, and E.Winter, "Phenomonology considerations for hyperspectral mine detection," in *Detection Technologies for Mines and Mine-like Targets*, A.C.Dubey, I.Cindrich, J. Ralston, and K.Rigano, eds., *Proc. SPIE* **2496**, pp. 159–167, 1995.